

Kent Academic Repository

Full text document (pdf)

Citation for published version

Hu, Yonghui and Yan, Yong and Efstratiou, Christos and Vela-Orte, David (2020) Quantitative Shape Measurement of An Inflatable Rubber Dam Using Inertial Sensors. In: 2020 IEEE International Instrumentation and Measurement Technology Conference (I2MTC), 25-28 May 2020, Dubrovnik, Croatia.

DOI

Link to record in KAR

<https://kar.kent.ac.uk/83762/>

Document Version

Author's Accepted Manuscript

Copyright & reuse

Content in the Kent Academic Repository is made available for research purposes. Unless otherwise stated all content is protected by copyright and in the absence of an open licence (eg Creative Commons), permissions for further reuse of content should be sought from the publisher, author or other copyright holder.

Versions of research

The version in the Kent Academic Repository may differ from the final published version.

Users are advised to check <http://kar.kent.ac.uk> for the status of the paper. **Users should always cite the published version of record.**

Enquiries

For any further enquiries regarding the licence status of this document, please contact:

researchsupport@kent.ac.uk

If you believe this document infringes copyright then please contact the KAR admin team with the take-down information provided at <http://kar.kent.ac.uk/contact.html>

Quantitative Shape Measurement of An Inflatable Rubber Dam Using Inertial Sensors

Yonghui Hu
School of Engineering and Digital Arts
University of Kent
Canterbury, Kent CT2 7NT, U. K.
Y.Hu-261@kent.ac.uk

Christos Efstratiou
School of Engineering and Digital Arts
University of Kent
Canterbury, Kent CT2 7NT, U. K.
C.Efstratiou@kent.ac.uk

Yong Yan
School of Engineering and Digital Arts
University of Kent
Canterbury, Kent CT2 7NT, U. K.
Y.Yan@kent.ac.uk

David Vela-Orte
Dyrhoff Limited
Folkestone, Kent CT19 4RJ, U. K.
david.vela@dyrhoff.co.uk

Abstract—Shape measurement is of great importance for the effective control and safe operation of inflatable rubber dams. This paper presents for the first time a method to measure the cross-sectional shape of a rubber dam by placing an array of inertial measurement units (IMUs) on the peripheral of the rubber dam. The IMU array measures tangent angles of the dam peripheral by fusing accelerometer and gyroscope measurements. A continuous tangent angle function is derived by interpolating the tangent angles at discrete locations using a cubic spline. Finally, the shape is reconstructed by integrating the tangent angle function along the peripheral of the rubber dam. The performance of the measurement system is validated against a camera on a purpose-built test rig. Experimental results show that the measured and reference shapes are very similar, with a maximum similarity index of 8.5% under typical conditions. In addition, it is demonstrated that the system is robust against node failure by excluding readings of faulty nodes from shape reconstruction.

Keywords—Inflatable rubber dam, shape measurement, inertial measurement unit (IMU), tangent angle, cubic spline.

I. INTRODUCTION

Rubber dams are flexible membrane structures placed across channels, streams and rivers as a substitute for traditional earth and concrete dams [1]. They can be inflated by air, water or the combination of both to raise the upstream water level and partially or completely deflated to allow passage of flood flows. In comparison with rigid hydraulic structures, rubber dams have numerous advantages, such as low cost, simple structure, long span, short construction time, easy maintenance, more earthquake resistant, etc. The application of rubber dams ranges from irrigation, water supply, hydropower generation, tidal barrier, flood control to recreation.

However, the flexibility of the rubber dam structures calls for continuous monitoring and control of their operating conditions. The cross-sectional shape and height of a rubber dam vary continuously with external water levels and internal pressures, the applied force of which on the dam are in turn functions of the former [2]. The loading-shape interaction poses significant challenges for the design, analysis and control of rubber dams. Air-filled rubber dams may exhibit V-notch behavior under low-pressure conditions, which makes it difficult to maintain a desired water level and flow rate [3]. In addition, rubber dams are prone to vibrate due to hydraulic

disturbances, which might damage or destroy the rubber membrane [4]. A Knowledge Transfer Partnerships (KTP) project was initiated between Dyrhoff Ltd and the University of Kent to develop a condition monitoring system that measures the cross-sectional shape, height and vibration of rubber dams. These parameters provide essential information for the effective control and safe operation of rubber dams. To the best of our knowledge, this system is the first of its kind in the rubber dam sector. This paper focuses on the measurement of the cross-sectional shape, from which the height of the rubber dam can be easily derived.

There exist several techniques available to measure the shape of structures. Non-contact methods based on stereo cameras and light detection and ranging (LiDAR) can reconstruct complex three dimensional (3D) surfaces with high resolution [5], but these systems require scanning of the measured object or installation of multiple cameras, which are difficult to implement in the field. Fiber Bragg grating (FBG) sensors are being increasingly applied for shape measurement of wind turbine blades, aircraft wings and soft robots due to advantages of small size, light weight, immunity to electromagnetic interference, resistance to corrosion, and multiple measuring points in one optical fiber [6]. However, the high cost, adverse temperature effects and sophistication of the system make this technique not well suited for the intended application in this project. Resistive flex and stretch sensors that are extensively used in wearable devices can measure bending or flexing based on the resistance across the sensor [7, 8]. Although they are simple, cheap, compact and robust, shortcomings such as nonlinearity, lower sensitivity and low accuracy restrict wider application of this technology. An array of MEMS (Microelectromechanical System) inertial sensors attached to the measured object can provide local orientation information for global shape reconstruction [9-12]. A few studies have used this technique for measurement of human spine postures and 3D shape sensing of flexible materials. Inertial sensors are small, cheap, power efficient, readily available and more importantly can also be used for vibration measurement. Therefore, the inertial sensing technique is used in this project for simultaneous shape, height and vibration measurement of rubber dams.

In this paper, the working principle, practical design and implementation of the prototype condition monitoring system are presented. A shape reconstruction algorithm is designed and the performance of the system is experimentally evaluated. Finally, some practical issues regarding the application of the system in the field are discussed.

The authors wish to acknowledge Innovate UK for providing financial support for this project (No. 1025486).

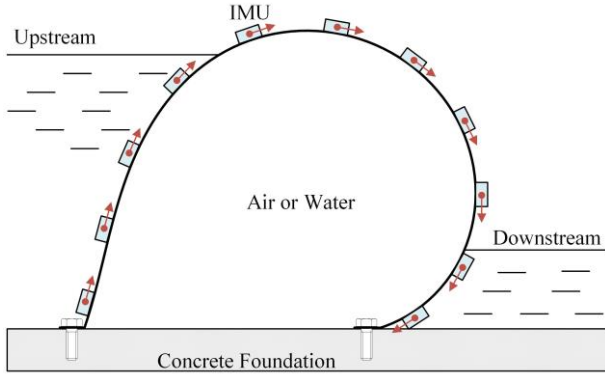


Fig. 1. Overall sensing arrangement and principle of the measurement system.

II. MEASUREMENT PRINCIPLE AND SYSTEM DESIGN

A. Overall Sensing Arrangement

A rubber dam consists of a sheet of rubber-coated fabric that is fixed to a reinforced concrete foundation using clamp plates and anchor bolts. When inflated, the rubber dam forms a shape of a teardrop, which depends on the external water levels and internal pressures. A number of analytical and numerical methods can be used to determine the cross-sectional shape of the rubber dam under given conditions [2, 3, 13]. In order to measure the shape of the rubber dam using the inertial sensing technique, an array of inertial measurement units (IMUs) with known distance between adjacent nodes is placed on the peripheral of the rubber dam. Based on the tangent angles measured by the IMUs, the shape of the rubber dam can be reconstructed numerically using an appropriate algorithm. Fig. 1 illustrates the overall sensing arrangement and principle of the measurement system. It is worth noting that the nodes of the IMU array are not necessarily equidistant, which implies that the system is able to tolerate failures of nodes with outlier readings.

B. Tangent Angle Measurement

In recent years, compact, low-cost MEMS inertial sensors have become commonly available for a broad range of industrial, biomedical and consumer applications. A 3-axis MEMS accelerometer can be used to determine attitude angles by measuring the direction of gravity under quasi-static conditions. For dynamic applications, the attitude measurement is corrupted by vibrations and impacts. By contrast, the angular velocity measured by a MEMS gyroscope can be integrated to derive accurate attitude measurements for short term. The accumulation of the gyroscope bias and noise over time leads to significant drift of the measured attitude. In order to obtain reliable attitude angles, IMUs that fuse together triaxial accelerometer and gyroscope measurements using an embedded sensor fusion algorithm are developed.

A number of sensor fusion algorithms for attitude estimation can be found in the literature, among which the extended Kalman filter (EKF) [14], the explicit complementary filter [15] and the optimized gradient descent algorithm [16] are most popular. The EKF is the de facto standard for nonlinear state estimation but requires high computational resources, whereas the latter two are simple and computationally efficient. In this paper, the explicit complementary filter is implemented on the embedded microcontroller of the IMU. This algorithm combines

accelerometer output for low frequency attitude estimation with integrated gyroscope output for high frequency estimation. Specifically, the attitude is derived by numerically integrating the following quaternion kinematic differential equation [15]:

$$\dot{\hat{q}} = \frac{1}{2} \hat{q} \otimes \mathbf{p}(\bar{\Omega} + \delta) \quad (1)$$

where \hat{q} is a unit quaternion representing the estimated attitude, \otimes is the quaternion product operator, $\mathbf{p}(\cdot)$ converts a vector to a pure quaternion, $\bar{\Omega}$ represents the angular velocity measured by the gyroscope, and δ is used to correct the gyroscope bias and expressed as:

$$\delta = k_p e + k_I \int e \quad (2)$$

where k_p and k_I are proportional and integral gains, respectively, and e is the error between the measured gravitational direction \bar{v} using the accelerometer and the estimated gravitational direction \hat{v} :

$$e = \bar{v} \times \hat{v} \quad (3)$$

After the attitude quaternion \hat{q} is obtained, the roll angle ϕ and pitch angle θ can be respectively derived from:

$$\phi = \text{tg}^{-1} \frac{2(\hat{q}_2 \hat{q}_3 + \hat{q}_0 \hat{q}_1)}{1 - 2(\hat{q}_1^2 + \hat{q}_2^2)} \quad (4)$$

$$\theta = -\sin^{-1} 2(\hat{q}_1 \hat{q}_3 - \hat{q}_0 \hat{q}_2) \quad (5)$$

Since the ranges of the roll and pitch angles are $(-180^\circ, 180^\circ)$ and $(-90^\circ, 90^\circ)$, respectively, the IMUs are mounted in such a way that the x -axes of the IMUs, around which the roll angles are measured, point to the longitudinal direction of the rubber dam.

C. Shape Measurement

According to the theory of classical differential geometry [17], the shape of an inflated rubber dam can be described by a differentiable curve parameterized by arc length:

$$\alpha: [0, L] \rightarrow \mathbb{R}^2 \quad (6)$$

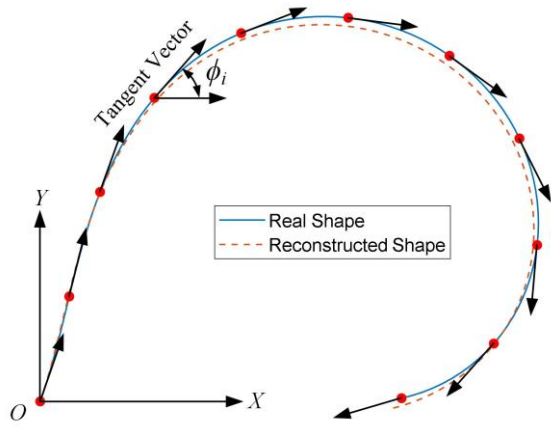
where L is the peripheral length of the rubber dam. The arc length is measured from the origin of the Cartesian coordinate system $O-XY$ in Fig. 2 (a), which corresponds to the anchor point at the upstream side in Fig. 1. The tangent vector of the curve α at arc length s is expressed as

$$\alpha'(s) = [\cos \phi(s), \sin \phi(s)] \quad (7)$$

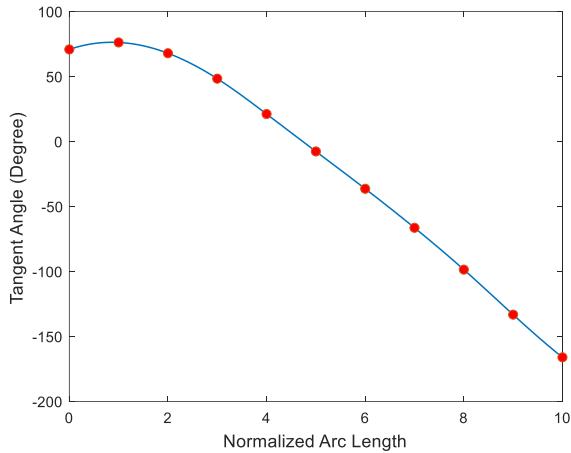
which is a unit vector making an angle $\phi(s)$ with the X -axis, as shown in Fig. 2(a). The tangent angle ϕ_i measured at s_i by the i -th ($i=1, 2, \dots, n$) IMU can be regarded as a sample of the continuous tangent angle function $\phi(s)$. Therefore, a natural cubic spline that interpolates the measurement points with piecewise polynomials is used to represent $\phi(s)$ [12], as shown in Fig. 2(b). The first and second derivatives of a cubic spline are continuous at the knots, which guarantees the smoothness of the curve. Once the analytical expression of $\phi(s)$ is obtained, the curve can be reconstructed by integrating the tangent vector:

$$\alpha(s) = \left[\int_0^s \cos \phi(t) dt, \int_0^s \sin \phi(t) dt \right] \quad (8)$$

Fig. 2(a) illustrates the shape of the rubber dam reconstructed numerically using the above algorithm.



(a) Real and reconstructed shapes.



(b) Interpolation of the tangent angles using a cubic spline.

Fig. 2 Reconstruction of the dam shape.

D. System Design and Implementation

The measurement system consists of an IMU array and a host PC that are serially connected by a RS485 bus and a power cable, as illustrated in Fig. 3. The number of IMUs depends on the peripheral length of the rubber dam and the desired accuracy of shape reconstruction. A USB-to-RS485 converter allows the IMUs to be connected to and powered by an USB port of the PC, which retrieves the measurement results of the IMUs successively using the Modbus RTU protocol. A console program that implements the shape measurement algorithm and visualizes the reconstructed shape on the PC was developed using Microsoft Visual C# .NET. For industrial applications, the IMU array will be connected to an on-site programmable logic controller (PLC) instead of a PC. The shape measurement results can thus be used for control of the internal pressure of the rubber dam.

The IMU shown in Fig. 3 is a custom-made sensor module using the latest off-the-shelf devices. The onboard MEMS inertial sensor is MPU6050 that combines a 3-axis gyroscope and a 3-axis accelerometer on a single chip. The sensor readings are accessed via a I2C interface by a microcontroller STM32F103C8T6 that features a 32-bit ARM Cortex-M3 core running at 72 MHz. The +5 V power supply from the USB port is regulated to +3.3 V using a low dropout regulator MIC5207. A half-duplex RS485 transceiver SP3485 converts the logic level UART signals into RS485 differential level signals.

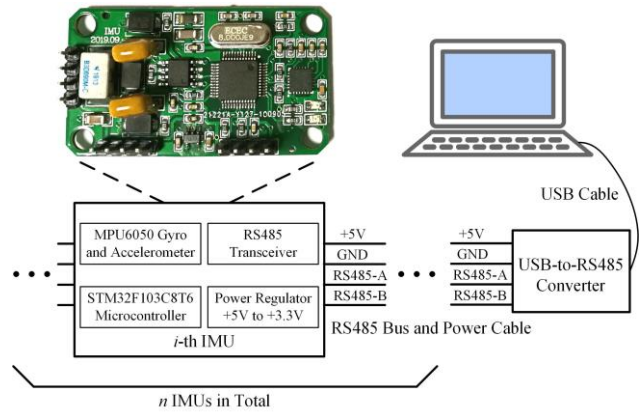


Fig. 3 Architecture of the measurement system.



Fig. 4 Test rig.

III. EXPERIMENTAL RESULTS AND DISCUSSION

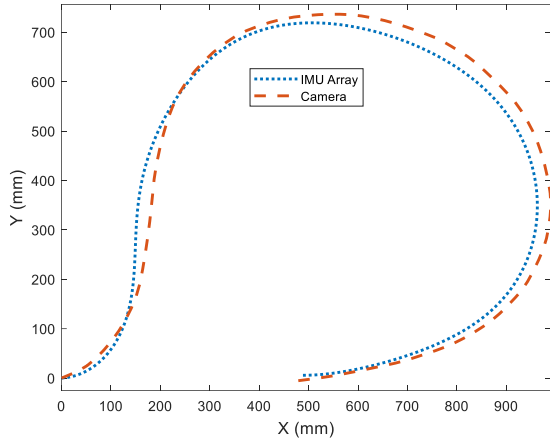
A. Experimental Setup

Experimental assessment of the shape measurement system was conducted on a purpose-built test rig, as shown in Fig. 4. An elastic steel strip with a dimension of 2284 mm \times 32 mm \times 0.6 mm (length \times width \times thickness) is used to simulate the cross section of the rubber dam. The IMUs are attached to the strip using screws with an equal spacing of 200 mm. The distances from the first and the last IMUs to both ends of the strip are 142 mm. The strip is fixed to a flat base plate at both ends, therefore the tangent angles at both ends are assumed to be 0° and 180° , respectively.

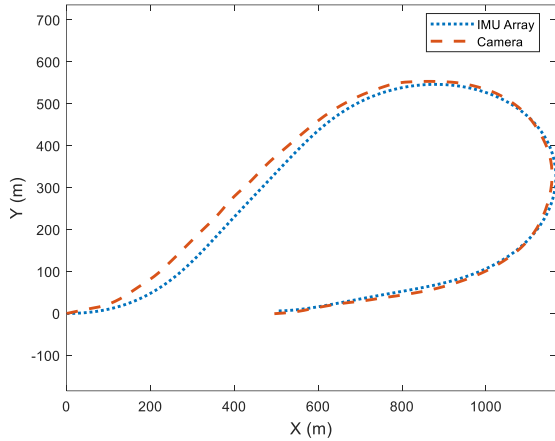
The steel strip was bended manually to form different shapes. In order to evaluate the shape measurement results quantitatively, the test rig was photographed using a digital camera mounted approximately on the central axis of the shape from a distance of 2.0 m. The digital image is processed using MATLAB and the steel strip is identified based on the color information. The dimension of the strip is then measured with the aid of an object with a known dimension in the image.

B. Shape Measurement Results

The IMU array was tested under different shapes of the steel strip. Fig. 5 shows two typical shapes that simulate dam cross-sectional shapes under high and low internal pressures, respectively. As illustrated, the shapes measured using the IMU array and the camera agree well with each other. A similarity index defined as the ratio of the area between the two shape curves to the area of the reference shape is used for quantitative assessment. The index is zero when the two shapes are exactly the same, and it may exceed one if the



(a) Shape under high internal pressure.



(b) Shape under low internal pressure.

Fig. 5 Shapes measured using the IMU array and the camera.

discrepancy is very large. For the shape measurement results in Fig. 5(a) and (b), the similarity indexes are 7.5% and 8.5%, respectively. In addition, the relative errors of height measurement are -2.4% and -1.3%, respectively. As can be seen in Fig. 4 and 5, the tangent angle at the upstream anchor point (the origin in Fig. 5) is not exactly zero as opposed to the aforementioned assumption, which leads to mismatch between both shapes at the upstream side. One shortcoming of the inertial sensing method for shape measurement is that the measurement error of one IMU node influences the overall shape because of the integration operation in equation (8). In the future, the test rig will be improved by using revolute joints and installing IMUs at the upstream and downstream anchor points in order to reduce the measurement errors.

As discussed above, this technique requires accurate measurement of the tangent angles by all IMU nodes. If one node is detected to be faulty or abnormal, the reading of this node should be discarded. In view of this, the influence of the number of nodes on the shape measurement results was investigated. Fig. 6 shows the shapes reconstructed without using one, three and five IMU nodes, respectively. As can be seen, when one node is discarded, the shape measurement result is affected only slightly. As more IMU nodes are discarded, the misclose between the measured and reference downstream anchor points increases. Nonetheless, the measured shape exhibits high similarity to the real shape even when five nodes are discarded. The similarity indexes for the three cases are 7.5%, 7.8% and 8.4%, respectively. It can thus

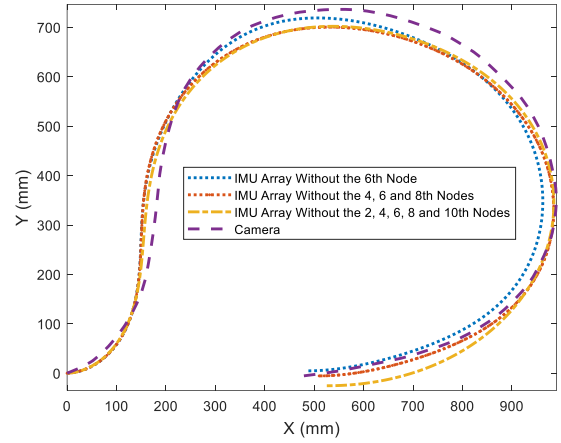


Fig. 6 Shapes measured without using some sensor nodes.

be concluded that more IMU nodes help increase the measurement accuracy, but a trade-off has to be made between accuracy and cost, system complexity as well as update rate that is subject to the communication bandwidth of the RS485 bus.

C. Discussion

The experimental results presented above were obtained under static conditions. It has been observed that under dynamic conditions the error of shape measurement increases considerably. This is because the external acceleration is superimposed on the gravitational acceleration and consequently causes uncertainty in attitude determination [18]. Since rubber dams experience vibrations under a variety of conditions, a new IMU algorithm that eliminates the attitude uncertainty should be designed in order to achieve accurate shape measurement under dynamic conditions.

Rubber dams vibrate at very low frequencies, i.e. a few Hz at maximum. It is feasible to animate the vibrating dam body on a computer screen using the shape measurement results at consecutive time instants. Vibration frequency and displacement can also be measured from the animation results. This provides a very convenient tool for operators to visually examine the condition of the rubber dam.

The measurement system will work in harsh underwater environments. Replacement of faulty sensor nodes is extremely difficult, if not impossible. Therefore, the validity of the sensor readings should be verified using some algorithm in order to avoid erroneous sensor readings to be used for shape reconstruction, as mentioned above.

Reliability is a major concern when scaling up the laboratory prototype to a full-scale industrial measurement system in the field, as rubber dams are safety critical hydraulic structures. A series of testing will be performed to discover potential problems in the field, such as electromagnetic compatibility (EMC) testing, ingress protection (IP) testing, thermal testing, etc.

IV. CONCLUSIONS

This paper has presented an inertial sensing based method to measure the cross-sectional shape of an inflatable rubber dam. Experimental results obtained have demonstrated that the measured and reference shapes agree well with each other, with a maximum similarity index of 8.5% under typical conditions. The measurement system enjoys a high degree of

fault tolerance by excluding erroneous IMU readings from shape reconstruction. Future work will focus on shape reconstruction under dynamic conditions, vibration measurement and assessment of the system in the field.

REFERENCES

- [1] X. Q. Zhang, P. W. M. Tam, and W. Zheng, "Construction, operation, and maintenance of rubber dams," *Canadian Journal of Civil Engineering*, vol. 29, no. 3, pp. 409-420, 2002.
- [2] M. Streeter, L. Rhode-Barbarigos, and S. Adriaenssens, "Form finding and analysis of inflatable dams using dynamic relaxation," *Applied Mathematics and Computation*, vol. 267, pp. 742-749, 2015.
- [3] N. Cheraghi-Shirazi, A. R. Kabiri-Samani, and B. Boroomand, "Numeric analysis of rubber dams using fluid-structure interactions," *Flow Measurement and Instrumentation*, vol. 40, pp. 91-98, 2014.
- [4] M. Gebhardt, "On the causes of vibrations and the effects of countermeasures at water-filled inflatable dams," *Proceedings of the First European Congress of the IAHR*, Edinburgh, UK, May 4-6, 2010.
- [5] G. Sansoni, M. Trebeschi, and F. Docchio, "State-of-the-art and applications of 3D imaging sensors in industry, cultural heritage, medicine, and criminal investigation," *Sensors*, vol. 9, pp. 568-601, 2009.
- [6] T. L. T. Lun, K. Wang, J. D. L. Ho, K. H. Lee, K. Y. Sze, and K. W. Kwok, "Real-time surface shape sensing for soft and flexible structures using fiber Bragg gratings," *IEEE Robotics and Automation Letters*, vol. 4, no. 2, pp. 1454-1461, 2019.
- [7] G. Saggio, F. Riillo, L. Sbernini, and L. R. Quitadamo, "Resistive flex sensors: a survey," *Smart Materials and Structures*, vol. 25, p. 013001, 2016.
- [8] A. Rashid and O. Hasan, "Wearable technologies for hand joints monitoring for rehabilitation: a survey," *Microelectronics Journal*, vol. 88, pp. 173-183, 2019.
- [9] G. D. Voinea, S. Butnariu, and G. Mogan, "Measurement and geometric modelling of human spine posture for medical rehabilitation purposes using a wearable monitoring system based on inertial sensors," *Sensors*, vol. 17, no. 1, p. 0003, 2017.
- [10] A. Dementyev, H. L. C. Kao, and J. A. Paradiso, "SensorTape: modular and programmable 3D-aware dense sensor network on a tape," *Proceedings of the 28th Annual ACM Symposium on User Interface Software & Technology*, pp. 649-658, Charlotte, NC, USA, November 11-15, 2015.
- [11] A. Hermanis, R. Cacurs, and M. Greitans, "Acceleration and magnetic sensor network for shape sensing," *IEEE Sensors Journal*, vol. 16, no. 5, pp. 1271-1280, 2016.
- [12] S. Nathalie, D. Dominique, L. Bernard, and B. Luc, "Curve reconstruction via a ribbon of sensors," *Proceedings of the 14th IEEE International Conference on Electronics, Circuits and Systems*, pp. 407-410, Marrakech, Morocco, December 11-14, 2007.
- [13] A. A. N. Alhamati, T. A. Mohammed, J. Norzaie, A. H. Ghazali, and K. K. Al-Jumaily, "Behavior of inflatable dams under hydrostatic conditions," *Suranaree Journal of Science and Technology*, vol. 12, no. 1, pp. 1-18, 2005.
- [14] A. M. Sabatini, "Quaternion-based extended Kalman filter for determining orientation by inertial and magnetic sensing," *IEEE Transactions on Biomedical Engineering*, vol. 53, no. 7, pp. 1346-1356, 2006.
- [15] R. Mahony, T. Hamel, and J. M. Pflimlin, "Nonlinear complementary filters on the special orthogonal group," *IEEE Transactions on Automatic Control*, vol. 53, no. 5, pp. 1203-1218, 2008.
- [16] S. O. H. Madgwick, A. J. L. Harrison, and R. Vaidyanathan, "Estimation of IMU and MARG orientation using a gradient descent algorithm," *Proceedings of 2011 IEEE International Conference on Rehabilitation Robotics*, pp. 179-185, Switzerland, June 29-July 1, 2011.
- [17] A. Pressley. *Elementary Differential Geometry*, 2nd Edition. Springer-Verlag London Limited, 2010.
- [18] J. K. Lee and M. J. Choi, "Robust inertial measurement unit-based attitude determination Kalman filter for kinematically constrained links," *Sensors*, vol. 19, no. 4, p. 768, 2019.